Compact Model of the Ballistic Subthreshold Current in Independent Double-Gate MOSFETs

D. Munteanu*, M. Moreau*, J.L. Autran*,**

* *L2MP-CNRS, UMR CNRS 6137, 49 rue Joliot-Curie, 13384 Marseille, France*
** *University Institute of France (IUF), 75000 Paris, France*
E-mail: daniela.munteanu@l2mp.fr, Phone: +33 4 96 13 98 19, Fax: +33 4 96 13 97 09

ABSTRACT

We present an analytical model for the subthreshold characteristic of ultra-thin Independent Double-Gate transistors working in the ballistic regime. This model takes into account short-channel effects, quantization effects and source-to-drain tunneling (WKB approximation) in the expression of the subthreshold drain current. Important device parameters, such as off-state current or subthreshold swing, can be easily evaluated through this full analytical approach. The model can be successfuly implemented in a TCAD circuit simulator for the simulation of IDG MOSFET based-circuits.

Keywords: Independently Driven Double-Gate MOSFET, ballistic transport, quantum effects, subthreshold current model

1 INTRODUCTION

Double-Gate (DG) MOSFETs are extensively investigated because of their promising performances with respect to the ITRS specifications for deca-nanometer channel lengths. In spite of excellent electrical performances due to its multiple conduction surfaces, conventional DG MOSFET allows only three-terminal operation because the two gate electrodes, i.e. the front gate and the back gate, are generally tied together. DG structures with independent gates have been proposed [1]-[2], allowing a four terminal operation. Independent Double-Gate (IDG) MOSFETs offer additional potentialities, such as a dynamic threshold voltage control by one of the two gates, transconductance modulation, signal mixer, in addition to the conventional switching operation. Thus, IDG MOSFETs are promising for future high performance and low power consumption very large scale integrated circuits. However, one of the identified challenges for IDG MOSFET optimization remains the development of compact models [3]-[6] taking into account the main physical phenomena governing the devices at this scale of integration. In this work, an analytical subthreshold model of ultra-thin IDG MOSFETs working in the ballistic regime is presented. The present approach captures the essential physics of such ultimate devices: short-channel effects, quantum confinement, thermionic current and tunneling of carriers through the source-to-drain barrier. Important device parameters, such as the off-state current (I_{off}) or the subthreshold swing, can be easily evaluated through this full analytical approach which also provides a complete set of equations for developing equivalent-circuit model used in ICs simulation.

2 DRAIN CURRENT MODELING

Figure 1 shows the schematic n-channel IDG MOSFET considered in this work. Carrier transport in the ultra-thin silicon film (thickness t_{Si}) is considered 1D in the x-direction and the resulting current is controlled by both the front and back gate-to-source (V_{G1} and V_{G2}) and drain-to-source (V_D) voltages which impact the shape as well as the amplitude of the source-to-drain energy barrier. In the subthreshold regime, minority carriers can be neglected and Poisson's equation is analytically solved in the x-direction with explicit boundary conditions at the two oxide/silicon interfaces taking into account the electrostatic influence of V_{G1} and V_{G2}. The expression of $\Psi(x)$ is obtained by applying the Gauss's law to the particular closed dashed surface shown in Fig. 1 [7]:

$$-E(x)\frac{t_{Si}}{2}+E(x+dx)\frac{t_{Si}}{2}-E_{S1}(x)=-\frac{qN_A t_{Si}dx}{2\varepsilon_{Si}} \qquad (1)$$

where E_{S1} is the electric field at the front interface given by:

$$E_{S1}=-\frac{(V_{FB1}-V_{FB2})-(V_{G1}-V_{G2})}{t_{Si}+2\gamma t_{ox}} \qquad (2)$$

where the electric field $E(x)\approx-\frac{d\psi(x)}{dx}$. After some algebraic manipulations, the following differential equation is obtained for the electrostatic potential in the silicon film:

$$\frac{d^2\Psi}{dx^2}-\frac{2C_{ox}}{\varepsilon_{Si}t_{Si}}\Psi=\frac{1}{\varepsilon_{Si}t_{Si}}\left[qN_A t_{Si}+2C_{ox}(V_{G1}-V_{FB1}-\phi_F)\right]+\frac{1}{\varepsilon_{Si}t_{Si}}\left[2C_{ox}(V_{G2}-V_{FB2}-\phi_F)\right] \qquad (3)$$

The solution of Eq. (3) is:

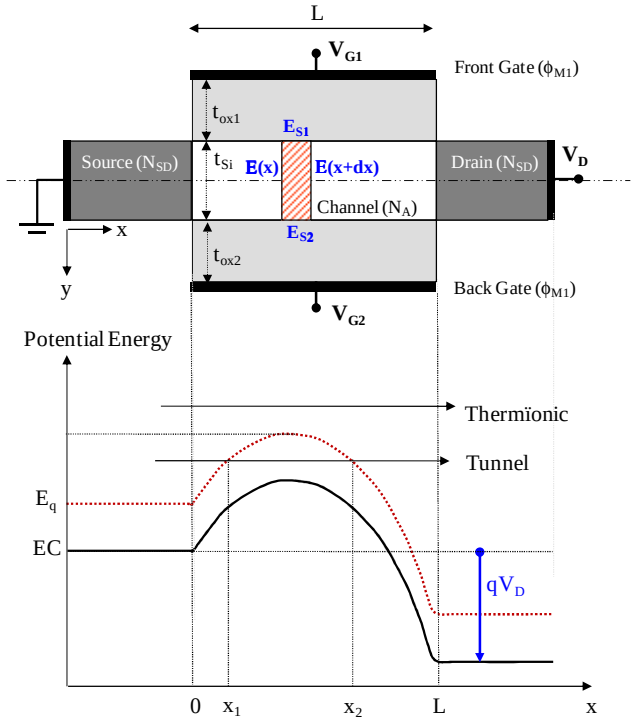

Figure 1: Schematic ultra-thin IDG MOSFET and its technological and electrical parameters considered in this work. The first energy subband profile $E_1(x)$ obtained from Eq. (9) is also represented (dotted line).

$$\psi(x) = C_1 \exp(\alpha x) + C_2 \exp(-\alpha x) - \frac{R}{\alpha^2} \tag{4}$$

where

$$C_{1,2} = \pm \frac{\phi_S\,[1-\exp(\mp\alpha L)] + V_D + R\dfrac{1-\exp(\mp\alpha L)}{\alpha^2}}{2\sinh(\alpha L)} \tag{5}$$

$$\alpha = \sqrt{\frac{2C_{ox}}{\varepsilon_{Si} t_{Si}}} \tag{6}$$

$$R = \frac{1}{\varepsilon_{Si} t_{Si}}\left(qN_A t_{Si} + 2C_{ox}(V_{G1} - V_{FB1})\frac{\gamma t_{ox} + t_{Si}}{2\gamma t_{ox} + t_{Si}}\right) + \frac{1}{\varepsilon_{Si} t_{Si}}\left(2C_{ox}(V_{G2} - V_{FB2})\frac{\gamma t_{ox}}{2\gamma t_{ox} + t_{Si}}\right) \tag{7}$$

$$\phi_S = \frac{kT}{q} ln\left(\frac{N_A N_{SD}}{n_i^2}\right) \quad \phi_F = \frac{kT}{q} ln\left(\frac{N_A}{n_i}\right) \quad \gamma = \frac{\varepsilon_{Si}}{\varepsilon_{ox}} \tag{8}$$

Considering the limit case of an ultra-thin Silicon film, we can assume only one energy subband for the vertical confinement of carriers. The first energy subband profile $E_1(x)$ can be easily derived as:

$$E_1(x) = q(\phi_S - \psi(x)) + E_q \tag{9}$$

where E_q is the first energy level calculated using the model developed in [8]:

$$E_q \cong \left(\frac{\hbar^2}{2m_l}\right) \times \left[\left(\frac{\pi}{t_{Si}}\right)^2 + A_l^2 \times \left(3 - \frac{4}{3}\frac{1}{1+(A_l t_{Si}/\pi)^2}\right)\right] \tag{10}$$

$$A_l \cong \left(\frac{3}{4} \times \frac{2m_l q E_{S1}}{\hbar^2}\right)^{1/3} \tag{11}$$

where m_l is the electron longitudinal effective mass (vertical confinement). Once $E_1(x)$ is known as a function of V_{G1}, V_{G2} and V_D, the total ballistic current (per device width unit) can be evaluated as follows:

$$I_{DS} = I_{Therm} + I_{Tun} \tag{12}$$

where I_{Term} and I_{Tun} are the thermionic and the tunneling components of the ballistic current, respectively. For a two-dimensional gas of electrons [9], I_{therm} and I_{tun} are given by:

$$I_{Therm} = \frac{2q}{\pi^2 \hbar}\int_{-\infty}^{+\infty} dk_z \times \int_{E_{1,max}}^{+\infty} [f(E,E_{FS}) - f(E,E_{FD})]dE_x \tag{13}$$

$$I_{Tun} = \frac{2q}{\pi^2 \hbar}\int_{-\infty}^{+\infty} dk_z \times \int_{0}^{E_{1,max}} [f(E,E_{FS}) - f(E,E_{FD})]T(E_x)dE_x \tag{14}$$

where $f(E_F,E_{FS})$ is the Fermi–Dirac distribution function, E_{FS} and E_{FD} are the Fermi-level in the source and drain reservoirs respectively ($E_{FD} = E_{FS} - qV_{DS}$), k_z is the electron wave vector component in the z direction, the factor 2 accounts for the two Silicon valleys characterized by m_l in the confinement direction (y-direction) and $T(E_x)$ is the barrier transparency for electrons and E is the total energy of carriers in source and drain reservoirs given by:

$$E = E_1 + E_x + \frac{\hbar^2 k_z^2}{2m_t} \tag{15}$$

where E_1 is the energy level of the first subband (given by Eq. (9)), E_x is the carrier energy in the direction of the current, m_t is the electron transverse effective mass. In Eq. (13) and Eq. (14) $E_{1,max}$ is the maximum of the source-to-drain energy barrier given by:

$$E_{1,max} = E_1(x_{max}) \tag{16}$$

where x_{max} is obtained from Eq. 3 with the condition:

$$\frac{d\Psi(x)}{dx} = 0 \quad for \quad x = x_{max} \tag{17}$$

$$x_{max} = \frac{1}{2\alpha} ln\left(\frac{C_2}{C_1}\right) \tag{18}$$

In Eq. (14), the barrier transparency is calculated using the WKB approximation:

NSTI-Nanotech 2008, www.nsti.org, ISBN 978-1-4200-8505-1 Vol. 3

$$T(E_x) = exp\left(-2\int_{x_1}^{x_2}\sqrt{\frac{2m_t(E_1(x)-E_x)}{\hbar^2}}dx\right) \quad (19)$$

where x_1 and x_2 are the coordinates of the turning points (Fig. 1). x_1 and x_2 have literal expressions due to the analytical character of the barrier:

$$x_{1,2}(E_x) = \frac{1}{\alpha} ln\left[\frac{A \pm \sqrt{\Delta}}{2C_1}\right] \quad (20)$$

where the quantities A and Δ are defined as follows:

$$A = \phi_S + \frac{R}{\alpha^2} + \frac{E_q}{q} - \frac{E_x}{q} \quad (21)$$

$$\Delta = A^2 - 4C_1C_2 \quad (22)$$

The WKB approximation has the main advantage to be CPU inexpensive and reasonably accurate for channel lengths down to a few nanometers. Moreover, it has been shown in [10] that differences between results obtained considering the WKB approximation and full quantum treatment (tight-binding scheme) are surprisingly small (typically a few percents), which confers to the WKB approach a reasonable accuracy in the frame of the present analysis.

3 RESULTS AND MODEL VALIDATION

Figure 2 shows the first energy subband profile in the Si film calculated with the model in a L=10 nm intrinsic channel IDG MOSFET (t_{Si} = 2 nm, t_{ox} = 0.6 nm). In order to test the validity of the model, we compare these profiles with those obtained with a self-consistent Poisson-Schrödinger solver based on a real-space Non-Equilibrium Green's Function (NEGF) approach (DGGREEN2D [11]).

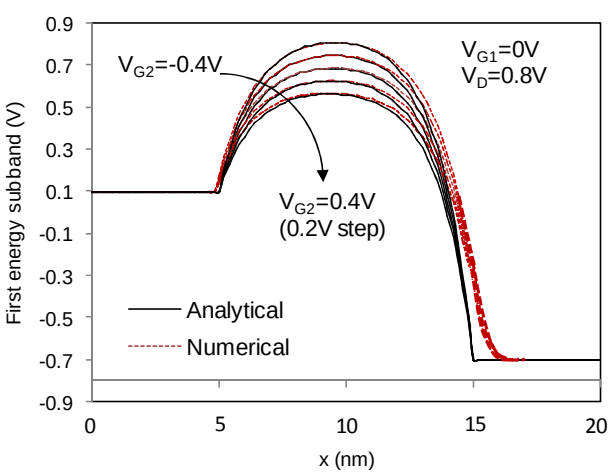

Figure 2: First energy subband profiles in the silicon film calculated with the analytical model (continuous lines) and with the 2D numerical code DGGREEN2D [11] (dotted lines). L=10 nm, V_D=0.8 V, V_{G1}=0 V.

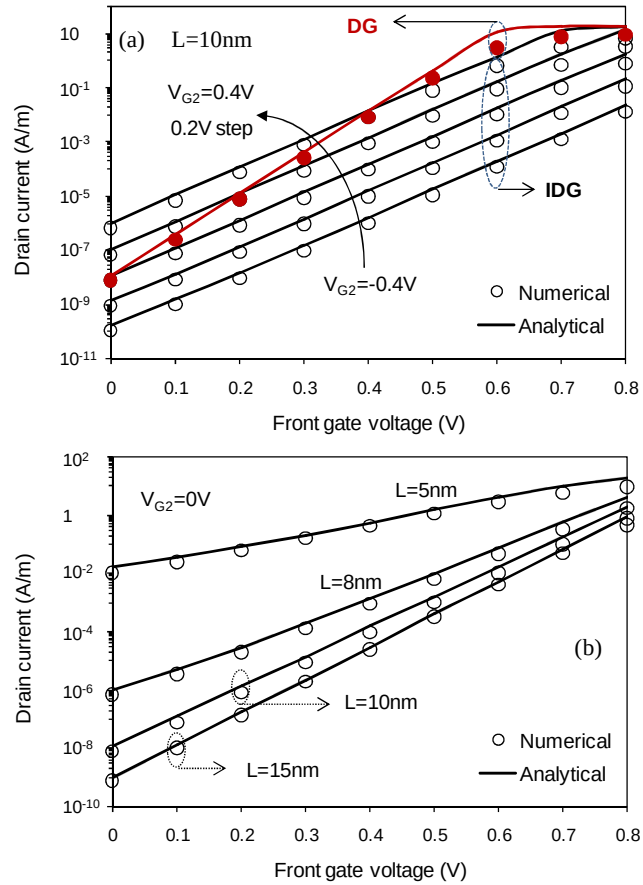

Figure 3: Subthreshold $I_{DS}(V_{G1})$ characteristics calculated with the analytical model (lines). Values obtained with the 2D numerical code DGGREEN2D [11] are also reported for comparison (symbols). DG=double-gate with connected gates. Other device parameters are the same as in Fig. 2.

As shown in Fig. 2 a good agreement is obtained between the two barriers in the subthreshold regime. In particular, we note an excellent agreement for the positions of the maximum as well as the amplitude of the barrier between the analytical and numerical curves. The slight difference in the barrier width is due to the electric field penetration in the source and drain regions, only taken into account in the numerical approach. Subthreshold $I_D(V_{G1})$ curves calculated with the analytical model are shown in Fig. 3a (for L = 10 nm and different V_{G2}) and Fig. 3b (for different channel lengths and V_{G2} = 0 V). The curves very well fit numerical data obtained with DGGREEN2D for devices in the deca-nanometer range.

4 DISCUSSION

In the following we use the proposed model to analyze the impact of source-to-drain quantum tunnelling on the IDG MOSFET operation. Figure 4 shows the source to drain energy barrier for different channel lengths. We note that below 8 nm the width of the channel barrier decreases

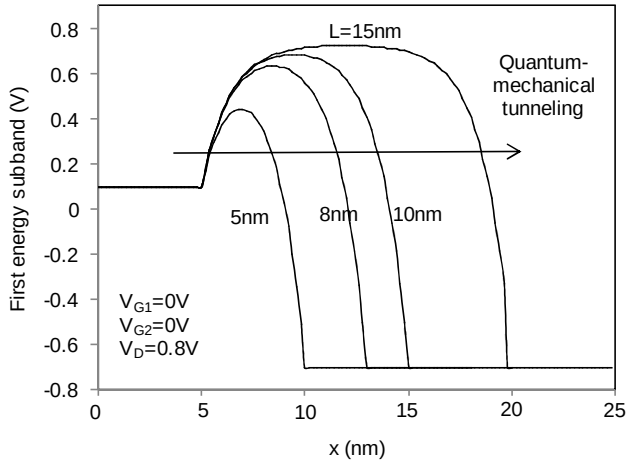

Figure 4: Variation of the source to drain energy barrier in the channel when decreasing the channel length (V_{G1}=V_{G2}=0 V, V_D=0.8 V).

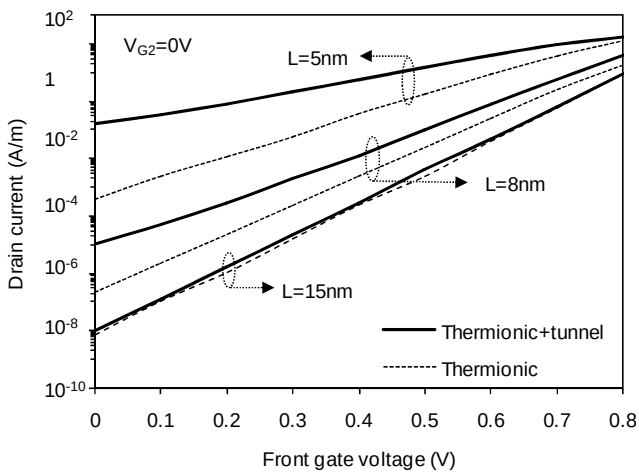

Figure 5: Subthreshold $I_D(V_{G1})$ characteristics calculated with the analytical model when considering or not the WKB tunneling component in the ballistic current. Device parameters are the same as in Fig. 2.

markedly, increasing the impact of the quantum tunneling on the device characteristics. We have analyzed the impact of carrier tunneling on device performances through a detailed comparison between simulations with and without quantum mechanical tunneling. Two cases are considered: (1) thermionic emission for $E_x > E_{max}$ and $T(E_x) = 0$ for $E_x < E_{max}$; (2) thermionic emission for $E_x > E_{max}$ and quantum tunneling with $T(E_x)$ given by the WKB approximation. Figure 5 shows subthreshold $I_D(V_{G1})$ characteristics calculated with the analytical model with and without WKB tunnelling component for channel lengths from 5 nm to 15 nm. These results highlight the dramatic impact of the source-to-drain tunneling on the subthreshold slope and also on the I_{OFF} current. In this subthreshold regime, the carrier transmission by thermionic emission is reduced or even suppressed due to the high channel barrier; as a consequence, when the channel length decreases the tunneling becomes dominant and constitutes the main physical phenomenon limiting the devices scaling, typically below channel lengths of ~ 8 nm. Quantum mechanical tunneling significantly degrades the off-state current especially in short channels, where the off-state current increases by more than two decades (L = 5 nm). However, the leakage current should be slightly reduced for the shorter geometries since it is calculated assuming perfectly ballistic transport and thus ignoring the partial reflection of electron wave functions on the source barrier. The subthreshold swing also increases (with about 30% for L = 8 nm with respect to L = 15 nm) due to quantum mechanical tunneling. As previously indicated for the leakage current, these results can be considered as an upper limit, since we assume perfectly ballistic transport without wave function reflection at the source barrier. Finally, the threshold voltage roll-off, is also notably affected by the carrier tunneling for channels shorter than 8 nm.

5 CONCLUSION

An analytical model for the subthreshold drain current in ultra-thin independent Double-Gate MOSFETs working in the ballistic regime is presented. The model is particularly well-adapted for ultra-short IDG transistors in the decananometer scale since it accounts for the main physical phenomena related to these ultimate devices: 2D short channel effects, quantum vertical confinement as well as carrier transmission by both thermionic emission and quantum tunneling through the source-to-drain barrier. The model is used to predict essential subthreshold parameters and can successfully be included in circuit models for the simulation of IDG MOSFET-based ICs.

Acknowledgements

This work was supported by the French Ministry of Research (ANR PNANO project “MULTIGRILLES”).

References

[1]. M. Masahara et al., IEEE Trans. El. Dev. **52** (2005) 2046.
[2]. L. Mathew et al., in Proc. IEEE Int. SOI Conf. 2004, 187.
[3]. W. Zhang et al., IEEE Trans. El. Dev., **52** (2005) 2198.
[4]. G. Pei and E.C. Kan, IEEE Trans. El. Dev. **51** (2004) 2086.
[5]. G. Pei et al., IEEE Trans. El. Dev., **50**, (2003) 2135.
[6]. X. Loussier et al., Proc. Nanotech-WCM 2006, p. 808.
[7]. D. Munteanu et al., Proc. Nanotech-WCM 2007, p. 574.
[8] V. Trivedi and J. Fossum, IEEE El. Dev. Lett. **26** (2005) 579.
[9]. D.K. Ferry and S.M. Goodnick. Cambridge University Press, 1997.
[10] M. Städele, in Proc.ESSDERC 2002, p. 135.
[11]. J.L. Autran and D. Munteanu, J. Comput. Theo. Nanosci. (2007), in press.